

The Binuclear Copper State of Peptidylglycine Monooxygenase Visualized through a Selenium- Substituted Peptidyl-Homocysteine Complex

Evan F. Welch§, Katherine W. Rush§†, Karsten A. S. Eastman‡, Vahe Bandarian‡ and Ninian J. Blackburn§*

§Department of Chemical Physiology and Biochemistry, Oregon Health and Sciences University, Portland, OR 97239

† Department of Chemistry and Biochemistry, Auburn University, Auburn, AL 36849 USA

‡Department of Chemistry, University of Utah, Salt Lake City, UT 84112, USA

Supplementary Information

Figure S1. Purification and characterization of the selenium-containing peptide Ala-Ala-Phe-homoselenocysteine (AAF-hSeCys). (a) HPLC chromatograph (b) mass spectrum showing $z=1$ and $z=2$ ions and (c) an expanded view of the $z=1$ and $z=2$ isotope distribution.

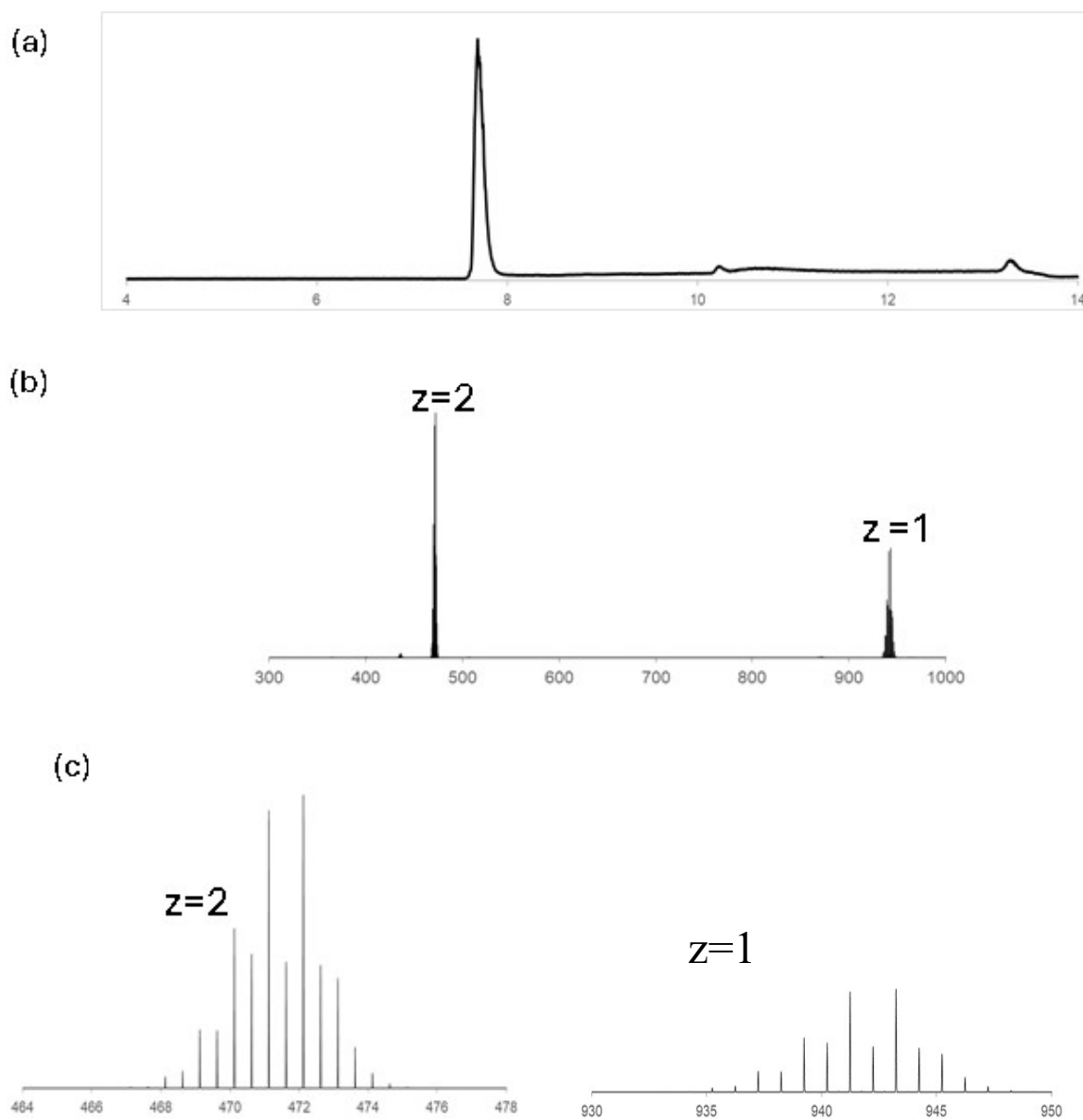


Figure S2. Exploration of the ability of various reductants to reduce the diselenide of AAF-hSeCys using X-ray absorption spectroscopy. The intensity of the Se-Se shell in the Fourier transform was compared for dithiothreitol (DTT), tricarboxyethylphosphine (TCEP), sodium borohydride, and sodium dithionite. The extent of reduction is indicated by the decrease in the intensity of this Se-Se interaction. (a) 1 mM AAF-hSeCys in 20 mM phosphate buffer pH 7.5 was treated with 10 mM each of DTT, TCEP and NaBH₄ (b) 1 mM AAF-hSeCys was treated with increasing concentrations of sodium dithionite.

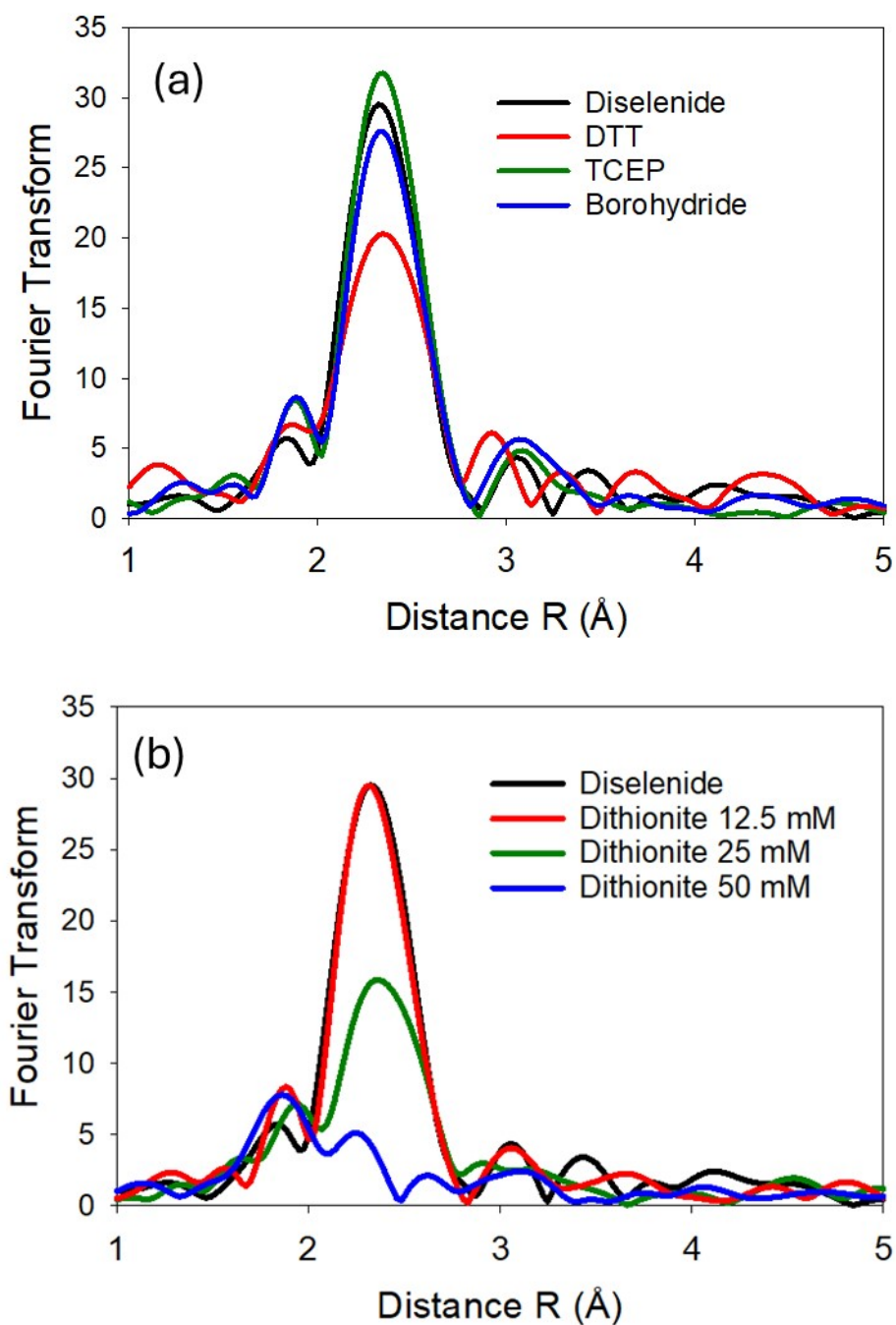


Figure S3. Effect of various added reductants on the enzyme activity of peptidylglycine monooxygenase (PHM). Reactions were performed, in 2 ml of buffered solution (50 mM MES pH 5.5, 30 mg / ml catalase, 25 μM CuSO_4 , 100 μM acetyl-YVG substrate) with 1 μM PHM. Reactions were initiated by adding 10 μl of 2 M ascorbate. The reagent to be tested was added after the oxygen had decreased to ~ 50 percent. Panels represent conditions as follows (a) no added reductant (b) 5 mM DTT. Panels (c) – (e) tested the effect of borohydride and its removal by quenching with TFA. Three separate reactions were performed. In the first reaction, normal enzyme activity was assessed with no additional additives, resulting in complete deoxygenation of the buffer over the course of approximately 5 minutes. In the second experiment, after approximately half the oxygen was consumed a small volume of concentrated borohydride in DMSO was added to a final concentration of 50 μM . The reaction was instantly arrested, accompanied by the formation of hydrogen gas. In the final reaction, after approximately half the oxygen was consumed a small volume of concentrated borohydride in DMSO quenched with 1 molar equivalent of TFA was added to a final concentration of 50 μM , resulting in no reaction.

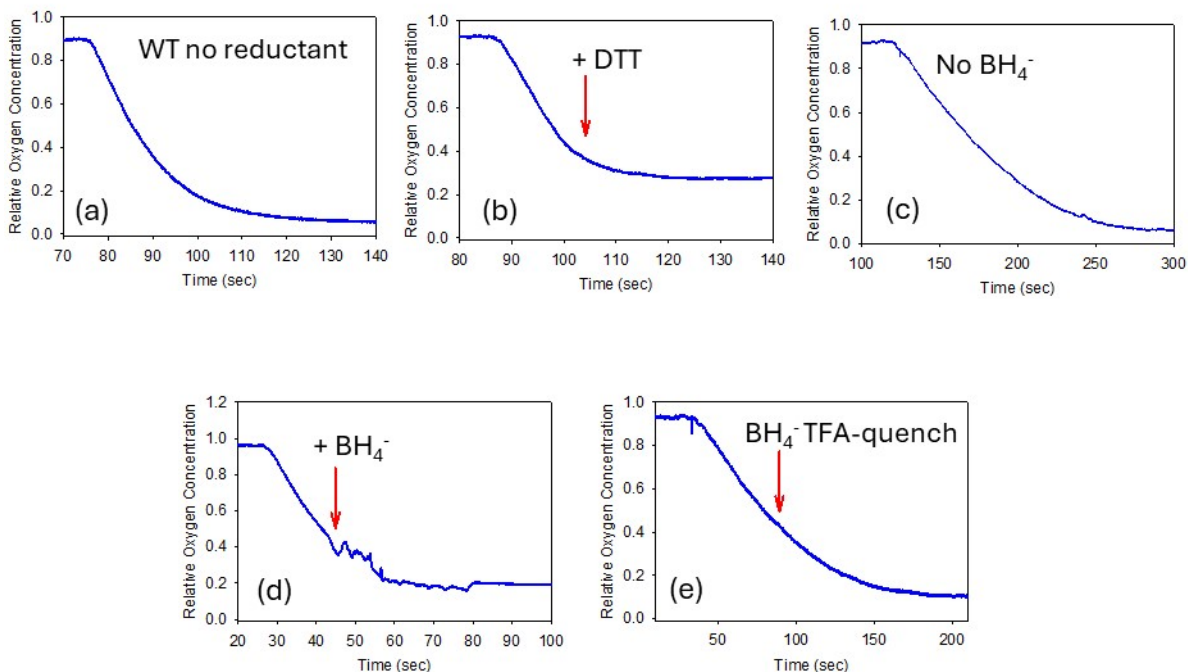


Figure S4. Reaction of oxidized PHM with AAF-SeM.

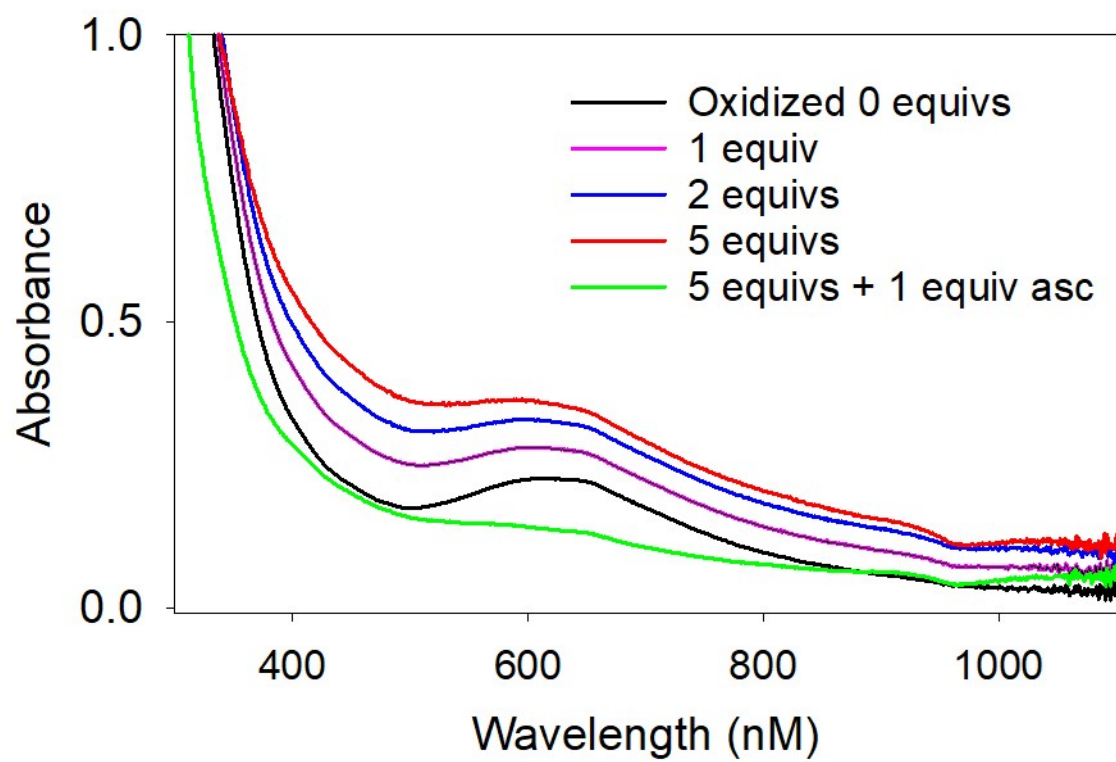


Table S1. Parameters used in the fits to EXAFS data of PHM reacted with 1 and 2 equivalents of AAF-hSeCys prepared by reduction with equimolar sodium borohydride followed by quenching with TFA.

Selenium edge		Se-C			Se-Se			Se-Cu			
	F¹ (x10⁻³)	No²	R (Å)³	DW (Å²)⁴	No	R (Å)	DW (Å²)	No	R (Å)	DW (Å²)	ΔE₀
2 equivalents		1	1.95	0.002	0.4	2.31	0.005	1.2	2.39	0.006	-2.4
Copper edge		Cu-N(His)⁵			Cu-S			Cu-Se			
	F (x10⁻³)	No	R (Å)	DW (Å²)	No	R (Å)	DW (Å²)	No	R (Å)	DW (Å²)	ΔE₀
1 equivalent	0.58	2	1.91	0.011	0.5	2.20	0.005	0.3	2.40	0.007	2.3
2 equivalents	0.57	2	1.92	0.017	0.5	2.20	0.004	0.6	2.40	0.007	3.5

$$F^2 = \frac{1}{N} \sum_{i=1}^N k^6 (Data - Model)^2$$

¹ F is a least-squares fitting parameter defined as $F = \sqrt{\frac{1}{N} \sum_{i=1}^N k^6 (Data - Model)^2}$. The larger value of F for Se arises from data ⁶

² Coordination numbers are generally considered as accurate +/- 25% unless indicated as low confidence.

³ In any one fit, the statistical error in bond-lengths is ±0.005 Å. However, when errors due to imperfect background subtraction, phase-shift calculations, and noise in the data are compounded, the actual error is probably closer to ±0.02 Å.

⁴ Debye-Waller (DW) factors are reported as 2σ² and are defined as twice the mean square deviation of the experimental bond distance as compared to the simulated value.

⁵ Imidazole rings were simulated using full multiple scattering from C2/C5 at 127° and C3/N4 at 163° from the Cu-N axis. Cu-C2/C5 = 2.78, 3.01 Å; Cu-N4/C5 = 4.03, 4.21 Å. The split shells approximate the average distortion of the imidazole plane from the Cu-N axis.

Table S2. Titration of oxidized PHM with selenopeptide. Four different titrations were carried out. Sample 1 was saved and used for EXAFS studies. Samples 2 – 4 were used for EPR quantitation and analysis as described in the text. Data for sample 4 is reported in Figure 6 with simulation parameters in Table S3. Extinction coefficients for the mixed-valence complex were calculated as follows. For samples taken at the titration end point before any ascorbate reduction, the difference between the total copper concentration and the Cu(II) component derived from the EPR detectable copper was presumed to be the Cu(I) component of the mixed valence complex. For the sample analyzed after ascorbate reduction, the EPR sample was thawed, the OD at 1000 nm measured, and the concentration of EPR detectable copper was now used as the concentration of MV complex, since ascorbate was deemed to have reduced all of the Cu(II) not contained in the MV. These calculations led to 3 independent measurements of the MV extinction coefficient as shown in the Table which average to $516 \pm 16 \text{ M}^{-1} \text{ cm}^{-1}$.

Sample	[Cu _{total}] (μM)	Equivalents selenopeptide at $\lambda_{\text{max}}=1000 \text{ nm}$	Max Abs at 1000 nm	[Cu(II)] (μM) from EPR	[MV] (μM)	Extinction coeff MV ($\text{M}^{-1}\text{cm}^{-1}$)	Percent EPR detectable
1	1000	3.0	0.60	N/A	N/A		N/A
2	580	4.0	0.51	305	275	539	53
3	1200	3.0	0.65	391	N/A		32
4	659	2.5	0.81	455	408	504	69
+ 5 mM Asc	572		0.49	124	248	506	21

Table S3. EPR parameters used in the fits to the unreacted oxidized PHM, mixed valence species, and mixed-valence species treated with 5 mM ascorbate and frozen immediately. Data correspond to sample 4 in Table S2. Spectra are averages of 4 scans and collected at a frequency of 9.396 GHz, 170K temperature, 2 mW microwave power, and amplitudes of 2, 6, and 10 Gauss depending on particular experimental conditions, as well as to assess the possibility of spectra broadening. Experimental data was simulated using EasySpin as described in the text. The spectrum of the mixed-valence species showing the position of the g_3 hyperfine peaks of both components is shown below the Table.

Sample	Component 1				Component 2				Ratio	rmsd
	g-value	A-value	Line Width	Strain	g-value	A-value	Line width	Strain		
PHM oxidized	g_1 2.071	A_1 30	3.7	g_3 0.04	g_1 2.085	A_1	8.0	g_3 0.04	1: 1	0.0231
	g_2 2.043	A_2 10		A_3 5	g_2 2.015	30		A_3 74		
	g_3 2.262	A_3 521			g_3 2.295	A_2 40				
					A_3 412					
Mixed-Valence	g_1 2.070	A_1 15	10.0	g 0.03	g_1 2.067	A_1 10	3.9	g_3 0.002	1: 0.8	0.0180
	g_2 2.058	A_2 25		A_3 0	g_2 2.017	A_2 5		A_3 227		
	g_3 2.258	A_3 531			g_3 2.288	A_3 409				
Mixed-Valence + ascorbate	g_1 2.060	A_1 20	3.2	g_3 0.004	g_1 2.104	A_1	4.60	g 0.05	1: 0.8	0.0114
	g_2 2.015	A_2 10		A_3 167	g_2 2.000	A_2 45		A_3 50		
	g_3 2.290	A_3 465			g_3 2.253	A_2 55				
					A_3 343					

